Synthesis and Characterization of Organoimido- and Organoamido-rhenium(v) Complexes. Crystal Structures of $[ReCl_2(NC_6H_4PPh_2\text{-}2)(HNC_6H_4PPh_2\text{-}2)]$, $[Re(8\text{-}HNC_9H_6N)_2O(PPh_3)][BPh_4]$ and $[Re(NPh)(NC_5H_3S\text{-}2\text{-}SiMe_3\text{-}3)_2(PPh_3)][BPh_4]$†

Mustafa T. Ahmet,[a] Brian Coutinho,[a] Jonathan R. Dilworth,*[a] John R. Miller,[a] Suzanne J. Parrott,[a] Yifan Zheng,[a] Mary Harman,[b] Michael B. Hursthouse[b] and Abdul Malik[b]

[a] *Department of Chemistry and Biological Chemistry, University of Essex, Wivenhoe Park, Colchester CO4 3SQ, UK*

[b] *School of Chemistry and Applied Chemistry, University of Wales, College of Cardiff, PO Box 912, Cardiff CF1 3TB, UK*

The reaction of $[ReCl_3O(PPh_3)_2]$ in toluene with 2-diphenylphosphinoaniline yielded the brown rhenium(v) amido/imido-complex $[ReCl_2(NC_6H_4PPh_2\text{-}2)(HNC_6H_4PPh_2\text{-}2)]$ **1**. This represents the first example of a metal complex where a 2-aminophenylphosphine is fully deprotonated to give an N,P chelated imido-complex. The crystal structure of **1** shows a distorted-octahedral geometry with the imido-nitrogen *trans* to chloride whereas the amido-nitrogen is disposed *trans* to a phosphorus. The Re–N length of 1.988(4) Å for the amido nitrogen is consistent with protonation of the nitrogen in the chelated ligand. A Re–N bond length of 1.757(4) Å and a Re–N–C angle of 137.8(3)° for the deprotonated imide nitrogen imply substantial multiple bonding. The oxo-complex $[Re(8\text{-}HNC_9H_6N)_2O(PPh_3)][BPh_4]$ **2** was the unexpected product in the reaction of $[ReCl_3O(PPh_3)_2]$ with 8-aminoquinoline in ethanol. It has a distorted-octahedral structure with two chelated amide ligands. The two quinoline-ring nitrogens as well as the two amido-nitrogens are arranged in a mutually *cis* configuration. The oxo and triphenylphosphine ligands occupy the remaining co-ordination sites. Reaction of $[ReCl_3(NPh)(PPh_3)_2]$ in ethanol with the sterically hindered 3-trimethylsilylpyridine-2-thiol (Htspyt) yielded the green rhenium(v) phenylimido-complex $[Re(NPh)(PPh_3)(tspyt)_2][BPh_4]$ **3**. Reaction of the unsubstituted pyridine-2-thiol (Hpyt) with the parent imido-complex yielded the analogous complex $[Re(NPh)(PPh_3)(pyt)_2][BPh_4]$ **4**. The crystal structure of **3** reveals a distorted-octahedral configuration of the ligands about the central rhenium atom. The imide and phosphine ligands are *cis* with the remaining sites being occupied by the S,N chelated pyridinethiolate ligands. A Re=N bond length of 1.725(8) Å and a Re–N–C bond angle of 166.0(6)° are indicative of the imide ligand functioning as a four-electron donor.

The organoimido core, M=N–R, could prove to be of great synthetic utility in radiopharmacology, since a variety of organic substituents can be incorporated into a stable rhenium– or technetium–nitrogen core. This allows chemical 'fine-tuning' of the biological properties of the complex by variation of the imido-core's organic substituent R, and this can be done independently of the other ligands on the metal. We here report our attempts to synthesise rhenium imido-complexes with enhanced stability, either by incorporation of the imide ligand into a chelate ring, or by the use of robust chelated co-ligands.

The first rhenium arylimido-complexes $[ReCl_3(NR)(PPh_3)_2]$ (R = aryl group) were reported by Chatt and Rowe[1] in 1962, using aniline as the source of the imide ligand. Syntheses of analogous alkylimido-complexes was subsequently reported.[2] Since then there have been several papers dealing with the substitution chemistry of these complexes to give derivatives such as $[PPh_4][Re(NPh)(SC_6H_2Pr^i_3\text{-}2,4,6)_4]$[3] or $[Re(NC_6H_4\text{-}Me\text{-}p)(OEt)(S_2CNEt_2)_2]$.[4] The latter is of interest as in contrast to the majority of structurally characterised mono-imido-complexes the Re–N–C angle is 155.5(5)°. This suggests a reduction in the formal number of electrons donated to the metal and a lower bond order. When the Re–N–C bond angle is close to 180° the imide ligand is regarded as donating four electrons.‡

A variety of other reagents has been used to introduce the imide ligand. The 2-arylazopyridines $YC_6H_4N{=}NC_5H_4N$ (Y = H, 3-Me, 4-Me or 4-Cl) undergo N=N bond cleavage on reaction with $K_2[ReCl_6]$ to give the imides $[ReCl_3(YC_6H_4N{=}NC_5H_4)(=NC_5H_4N)]$.[5] Several reports have appeared of the use of aryl isocyanates RNCO to prepare imides by reaction with oxo-complexes and elimination of CO_2. The anion $[ReCl_4O]^-$ reacts with PhNCO to give polymeric $[\{ReCl_4(NPh)\}_n]$ which forms adducts with a number of neutral two-electron-donor ligands.[6] This type of chemistry has subsequently been extended to the synthesis of the tris(imido)-complex $[ReMe(NBu^t)_3]$ from $[ReMeO_3]$.[7] It was found that the homoleptic tetrakis(imido)-complex $[Li(tmen)][Re(NBu^t)_4]$ (tmen = *N*,*N*,*N*′,*N*′-tetramethylethane-1,2-diamine) can be prepared by deprotonation of $[Re(NBu^t)_3(NHBu^t)]$ with butyllithium in the presence of tmen.[8]

Although the bis(imido)-complexes $[ReMeCl_2(NBu^t)_2(py)]$ (py = pyridine) are available by the addition of pyridinium halides to $[ReMe(NBu^t)_3]$,[7] a much more convenient route is

† *Supplementary data available:* see Instructions for Authors, *J. Chem. Soc., Dalton Trans.*, 1995, Issue 1, pp. xxv–xxx.

‡ Here the RN imide-ligand is taken to be neutral. If a dianionic charge is assumed then the formal number of electrons donated is six.

directly from Re_2O_7 by reaction with $SiMe_3Cl$ and pyridine in CH_2Cl_2.[9] This gives the readily derivatised complexes $[ReCl_3(NR)_2(py)]$ in high yield. The synthesis of imido-complexes directly from perrhenate is an essential step for any complex to have viability as a radiopharmaceutical, as $[ReO_4]^-$ (as ^{186}Re or ^{188}Re) is the sole precursor available from commercial generators. The use of 1-acyl-2-arylhydrazines for the preparation of imides from perrhenate in protic media will be discussed in a forthcoming paper.[10]

The major thrust for much of the recent work has been the quest for an efficient rhenium homogeneous catalyst for olefin or acetylene metathesis. Although $[Re(CHBu^t)(NR)_2\{OCMe(CF_3)_2\}_2]$ (R = 2,6-diisopropylphenyl) is virtually inert for metathesis catalysis, the related tungsten complex is very reactive.[11] However, the complexes $[Re(\equiv CBu^t)(NR)(OR')_2]$ (R = aryl, R' = variety of alkyl groups) metathesise acetylenes very efficiently. Although the complexes $[Re(CHBu^t)Cl_2(NR)(OR)]$ are themselves inert as metathesis catalysts, the addition of Lewis acids does generate a catalyst capable of metathesising hept-3-ene at about 1000 turnovers per minute.[12]

Imido-complexes in which the imide ligand is incorporated into a chelated system are much less common, the first example being $[ReCl(NC_6H_4CO_2\text{-}4)(OEt)(PPh_3)_2]$, prepared by reaction of $[ReCl_3O(PPh_3)_2]$ with 2-carboxyaniline in ethanol.[13] This complex was not however structurally characterised, and the reactivity of the chelated imide ligand will be discussed elsewhere.

Results and Discussion

Preparation and Properties of the Imido-complexes.—The rhenium(v) precursor $[ReCl_3O(PPh_3)_2]$ reacts readily with $2\text{-}Ph_2PC_6H_4NH_2$ in toluene under reflux to yield the brown, air-stable rhenium(v) complex $[ReCl_2(NC_6H_4PPh_2\text{-}2)(HNC_6H_4PPh_2\text{-}2)]$ **1** in near-quantitative yield. Reactions of transition-metal complexes with (2-aminophenyl)diphenylphosphine have previously solely formed organoamido-complexes. Such complexes include $[M(HNC_6H_4PPh_2\text{-}2)_2]$, where M = Pt[14] or Ni,[15] $[ReCl(HNC_6H_4PPh_2\text{-}2)_2O]$[16] and $[Tc(HNC_6H_4PPh_2\text{-}2)(H_2NC_6H_4PPh_2\text{-}2)_2][ClO_4]$.[17] The product formed is dependent on the rhenium precursor used, as the oxobis(amido) complex is formed from $[ReCl_4O]^-$.[16] In our reaction the PPh_3 liberated in the substitution reaction almost certainly removes the oxo-group as triphenylphosphine oxide, this being generally observed in the reactions of $[ReCl_3O(PPh_3)_2]$ with amino-compounds.

The ^1H NMR spectrum of complex **1** displays a complicated series of resonances in the range δ 6.1–7.8 attributable to the phenyl protons of both chelated phosphineaminobenzene ligands. The resonance for the protonated nitrogen is not observed, but an absorption in the infrared at 3260 cm^{-1}, indicative of N–H stretching, can be identified. The $^{31}P\text{-}\{^1H\}$ NMR spectrum shows two singlets indicative of two distinct and uncoupled phosphorus atoms. This observation is surprising in view of the crystal structure (see below) which indicates that both P atoms are co-ordinated and would therefore be expected to couple. It is possible that the coupling constant between the P atoms is 0, but it seems more probable that one of them is not co-ordinated. Moreover the shift of one of the phosphine resonances at δ −4 is close to the value of the 2-diphenylphosphinoaniline precursor at δ −5.5. If the P atom of the chelated imide ligand is not bound the ligand can function as a linear four-electron donor (RN regarded as neutral), giving a formal 18-electron count to the metal. Monodentate co-ordination of 2-substituted aryldiphenylphosphines has been observed in the solid state for the complex $[Re(SC_6H_4PPh_2\text{-}2)_3(MeCN)(PPh_3)]$.[18] The driving force for the change in co-ordination *in solution* for **1** may be the formation of a stronger, linear metal–nitrogen multiple bond. Possible structures in solution are shown in **A** and **B**. Both would explain the two phosphorus environments observed in the $^{31}P\text{-}\{^1H\}$ NMR spectrum and it is difficult at this stage to postulate the more likely configuration of the ligands. The fast atom bombardment mass spectrum of **1** shows the parent ion at m/z = 808. The fragment observed at m/z = 773 corresponds to loss of chloride to give the species $[ReCl(NC_6H_4PPh_2\text{-}2)(HNC_6H_4PPh_2\text{-}2)]^+$.

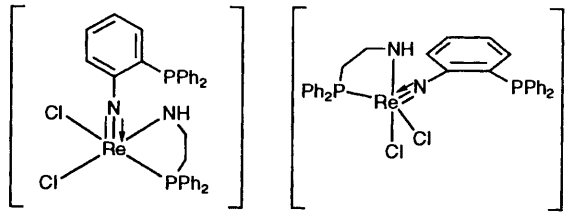

A **B**

The brown bis(8-amidoquinoline) complex $[Re(8\text{-}HNC_9H_6N)_2O(PPh_3)][BPh_4]$ **2** is prepared in high yield by reaction of $[ReCl_3O(PPh_3)_2]$ with 8-aminoquinoline under reflux in methanol. Even in the presence of an excess of aminoquinoline or added triethylamine there was no evidence for the formation of a chelated imide ligand analogous to that found for **1**. A recent paper by Bruce and co-workers[19] reported the attempted synthesis of an 8-imidoquinoline complex by reaction of 8-azidoquinoline with $[Mo(CO)_3(MeCN)_2(PPh_3)]$ which unexpectedly gave the phosphinimine complex $[Mo(CO)_4(Ph_3P{=}NC_9H_6N)]$. This is consistent with the intermediate formation of an imide with nitrene-like character. It appears that in the case of the higher-oxidation-state rhenium complex the 8-amino group is more basic than the corresponding 2-diphenylphosphinoaniline and cannot be deprotonated to give an imide ligand.

Complex **2** shows a strong IR band at 897 cm^{-1} assigned to ν(Re=O) and two weak sharp bands at 3314 and 3273 cm^{-1} are attributed to ν(N–H). The ^1H NMR spectrum is unremarkable, showing a complex multiplet in the range δ 6.6–8.0 due to the aromatic protons of the amidoquinoline and phosphine ligands and tetraphenylborate counter ion. The $^{31}P\text{-}\{^1H\}$ NMR spectrum shows the expected singlet at δ 4.4 due to the lone co-ordinated phosphine ligand. The FAB mass spectrum shows a peak at m/z = 751 with the appropriate isotope distribution. Another peak at m/z = 489 corresponds to loss of the PPh_3 ligand.

The rhenium(v) complex $[ReCl_3(NPh)(PPh_3)_2]$ reacts readily with 3-trimethylsilylpyridine-2-thiol (Htspyt) and pyridine-2-thiol (Hpyt) to yield the cationic green crystalline complexes $[Re(NPh)(PPh_3)(tspyt)_2][BPh_4]$ **3** and $[Re(NPh)(PPh_3)(pyt)_2][BPh_4]$ **4**, respectively. Both complexes were isolated as their tetraphenylborate salts. Co-ordination of the pyridinethiol ligand was confirmed by the observations of the IR stretching frequencies attributed to ν(NS) at 1550 and 1580 cm^{-1} in **3** and **4** respectively. The IR spectra also show strong IR absorptions at *ca.* 1160 cm^{-1} assigned to the C–S stretching mode of the co-ordinated thiolate. This is some 20 cm^{-1} higher than the stretching frequency for the free thiol indicating a partial increase in C–S bond order due to delocalisation. The ^1H NMR spectrum of **3** is unremarkable except for the two singlets due to the methyl protons of the silyl group which demonstrate rotation around the C–S bond. The stoichiometry of **3** is analogous to that of the unsubstituted pyridinethiolate complex **4** showing that the trimethylsilyl groups do not influence the mode of co-ordination. Zubieta and co-workers[20] have reported a number of unusual co-ordination geometries arising from the use of sterically hindered pyridinethiols.

Crystal and Molecular Structures.—A representation of the structure of complex **1** is shown in Fig. 1 along with the associated atom numbering scheme. Selected bond lengths and angles are given in Table 1. The overall geometry about the Re

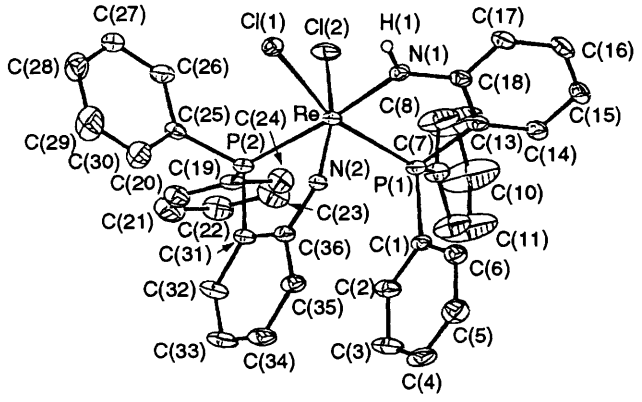

Fig. 1 Perspective view of $[ReCl_2(NC_6H_4PPh_2\text{-}2)(HNC_6H_4PPh_2\text{-}2)]$ **1** showing the atom labelling scheme

Table 1 Selected bond lengths (Å) and angles (°) for $[ReCl_2(NC_6H_4PPh_2\text{-}2)(HNC_6H_4PPh_2\text{-}2)]$ **1**

Re–N(1)	1.988(4)	Re–Cl(1)	2.405(1)
Re–N(2)	1.757(4)	Re–Cl(2)	2.388(1)
Re–P(1)	2.436(1)	N(1)–H(1)	0.78(5)
Re–P(2)	2.491(1)		
Re–N(1)–C(18)	126.5(2)	N(2)–Re–Cl(2)	157.1(1)
Re–N(2)–C(36)	137.8(3)	N(2)–Re–Cl(1)	98.6(1)
N(2)–Re–N(1)	107.2(2)	P(1)–Re–P(2)	105.06(4)
Re–N(1)–H(1)	109(3)	N(1)–Re–P(2)	174.8(1)
Re–P(1)–C(13)	99.8(1)	N(2)–Re–P(2)	75.4(1)
Re–P(2)–C(31)	98.8(1)	N(1)–Re–P(1)	79.7(1)
N(1)–Re–Cl(2)	95.3(1)		

is distorted octahedral, with the principal distortions coming from the relatively small bite angles of the chelated ligands, N(2)–Re–P(2) 75.4 and N(1)–Re–P(1) 79.7°. The amido-nitrogen N(1) is *trans* to P(2) of the chelated imide ligand, while the imido-nitrogen N(2) is *trans* to chloride Cl(2). The presence of the imide ligand is shown by the Re–N(2) length of 1.757(4) Å compared to the longer Re–N(1) 1.988(4) Å for the amide. The Re–N(2)–C(36) angle of 137.8(3)° is substantially larger than the corresponding Re–N(1)–C(18) 126.5(2)° for the amide ligand, reflecting the tendency for the M–N–C system to be closer to linear for the imide as the non-bonding electrons become involved in metal–nitrogen bonding. The bond parameters found for the chelated amide ligand are generally very similar to the values found for the bis(amido)-complex $[ReClO(HNC_6H_4PPh_2\text{-}2)_2]$.[16] The Re–P(2) length of 2.491(1) Å is significantly longer than the other Re–P length of 2.436(1) Å due to the steric strain induced by the opening of the Re–N(2)–C(36) angle. This lengthening is consistent with P(2) becoming dissociated in solution to give the N-bound imide ligand. The Re–N(2)–C(36) angle of 137.8(3)° for the chelated imide is close to the value of 139° found in the complex $[Mo(NPh)_2(S_2CNEt_2)_2]$.[21] The Re–N(2) length of 1.757(4) Å is also consistent with a metal–nitrogen bond order lower than the value of three usually encountered with linear imide ligands.

A representation of the structure of complex **2** appears in Fig. 2, together with an atom labelling scheme. Selected bond lengths and angles are in Table 2. Again the geometry is best described as distorted octahedral, the distortion being due to the presence of two chelated amide ligands. One amido-nitrogen is *trans* to an oxo-group, the other *trans* to the quinoline ring nitrogen of the other chelated amide ligand. Comparison of the bond lengths and angles of the chelated amide ligands in complexes **1** and **2** reveals that the quinoline-

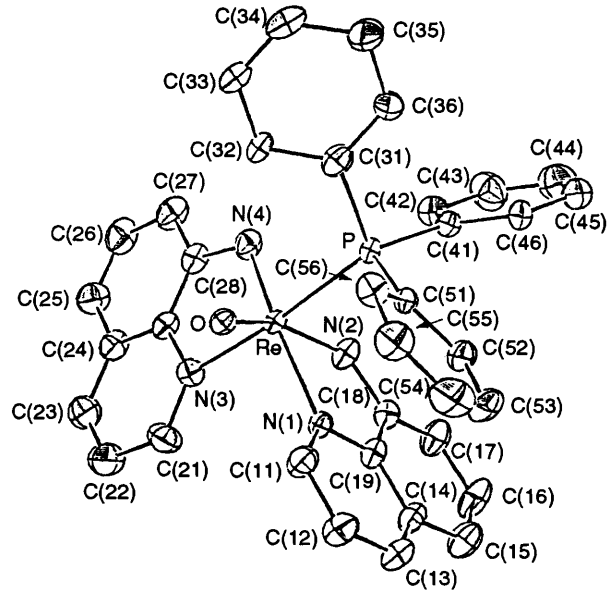

Fig. 2 Perspective view of $[Re(8\text{-}HNC_9H_6N)_2O(PPh_3)][BPh_4]$ **2** showing the atom labelling scheme

Table 2 Selected bond lengths (Å) and angles (°) for $[Re(8\text{-}HNC_9H_6N)_2O(PPh_3)][BPh_4]$ **2**

Re–P	2.441(2)	Re–N(2)	2.028(6)
Re–O	1.711(5)	Re–N(3)	2.157(6)
Re–N(1)	2.183(6)	Re–N(4)	1.958(6)
Re–N(1)–C(11)	126.3(5)	O–Re–N(2)	160.4(3)
Re–N(1)–C(19)	115.9(5)	O–Re–N(3)	90.9(3)
Re–N(3)–C(21)	128.1(5)	O–Re–N(4)	109.3(3)
Re–N(3)–C(29)	110.9(5)	N(1)–Re–N(2)	74.6(2)
P–Re–O	88.1(2)	N(1)–Re–N(3)	95.9(2)
P–Re–N(1)	89.8(2)	N(1)–Re–N(4)	164.1(2)
P–Re–N(2)	92.7(2)	N(2)–Re–N(3)	90.3(2)
P–Re–N(3)	174.2(2)	N(2)–Re–N(4)	90.1(3)
P–Re–N(4)	95.5(2)	N(3)–Re–N(4)	79.5(3)
O–Re–N(1)	85.8(2)		

ring nitrogen–rhenium lengths of 2.183(6) and 2.157(6) Å are shorter than the corresponding P–Re length of 2.436(1) Å while the Re–N (amide) bonds are similar in length. The Re–N(3)–C(29) angle of 110.9(5)° is much larger than the related angle in the phosphorus amide ligand [Re–P(2)–C(31) 98.8(1)°], and there is a corresponding decrease in the Re–N(1) (amide)–C(19) angle to 115.9(5)° for the quinoline amide compared to the Re–N(1) (amide)–C(18) angle of 126.5(2)° for the phosphinamide ligand. Since the other chelate ring angles are comparable, the principal difference appears to reside in the bond length to the non-amido-heteroatom in the ring. The dihedral angle between the two planes consisting of the quinoline rings was found to be very close to 90° at 93.55°.

The crystal structure of complex **3** is shown in Fig. 3, and selected bond lengths and angles are given in Table 3. The structural analysis shows the molecule to have distorted-octahedral geometry, the distortion being due to the small bite angles for the thiolate ligands, N(2)–Re–S(2) 65.6(2)° and N(1)–Re–S(1) 68.0(2)°. The Re–N(3) bond length of 1.725(8) Å and bond angle Re–N(3)–C(35) of 166.0(6)° are consistent with the imide ligand functioning as a linear four-electron donor. With reference to the Re–N(3) (imide) bond as a principal axis, one of the thiolate ligands occupies two equatorial sites while the second spans both equatorial and axial sites. The imide and phosphine ligands are disposed *trans* to the pyridyl nitrogens. The C–S bond lengths of 1.776(9) and 1.732(10) Å show partial

double-bond character as compared to a single bond length of 1.81 Å. This was reflected in the higher wavenumber observed for ν(C–S) in the infrared spectrum. The Re–N bond lengths of the pyridinethiolate ligands at 2.112(7) and 2.173(8) Å are typical for Re–N single bonds. Slight differences in overall metal–sulfur orbital overlap for the pyridinethiols are reflected in the differing bond lengths, Re–S 2.371(3) and 2.458(3) Å. The overall structure is similar to that found for $[ReL_2(NPh)(PPh_3)][BPh_4]$[22] [HL = maltol (3-hydroxy-2-methyl-4*H*-pyran-4-one)].

Table 3 Selected bond lengths (Å) and angles (°) for $[Re(NPh)(PPh_3)(tspys)_2][BPh_4]$ **3**

Re–P	2.436(3)	Re–N(3)	1.725(8)
Re–S(1)	2.371(3)	C(35)–N(3)	1.388(9)
Re–S(2)	2.458(3)	C(19)–S(1)	1.776(9)
Re–N(1)	2.112(7)	C(27)–S(2)	1.732(10)
Re–N(2)	2.173(8)		
Re–N(3)–C(35)	166.0(6)	N(3)–Re–S(2)	91.2(3)
S(1)–Re–P	93.4(9)	N(2)–Re–S(1)	90.6(2)
S(2)–Re–S(1)	152.49(9)	N(2)–Re–N(3)	156.7(3)
N(2)–Re–S(2)	65.6(2)	N(1)–Re–S(2)	93.8(2)
N(1)–Re–S(1)	68.0(2)	N(1)–C(19)–S(1)	106.6(6)
N(1)–Re–P	158.1(2)	N(2)–C(27)–S(2)	108.0(7)

Electrochemistry.—Cyclic voltammetry data for complexes **1–4** are summarised in Table 4. The cyclic voltammogram of $[ReCl_2(NC_6H_4PPh_2\text{-}2)(HNC_6H_4PPh_2\text{-}2)]$ **1**, Fig. 4(*a*), shows partially reversible oxidation and reduction processes, which were not found to become reversible at 200 K, confirming a rapid irreversible chemical reaction after electron transfer. The cyclic voltammogram of $[Re(8\text{-}HNC_9H_6N)_2O(PPh_3)][BPh_4]$ **2** is shown in Fig. 4(*b*). In the positive sweep an irreversible process was observed which corresponds to oxidation of the tetraphenylborate counter ion. A peak at an identical potential is observed in the cyclic voltammogram of sodium tetraphenyl-

Table 4 Cyclic voltammetric data* for complexes **1–4**

Complex	Process	i_{pa}/i_{pc}	E_{pa}/V	E_{pc}/V	E_p/mV	$E_{\frac{1}{2}}$/V
1	Oxidation	—	0.73	0.62	110	0.68
	Reduction	0.5	−1.36	−1.44	80	−1.40
2	Oxidation	—	0.57	—	—	
	Reduction 1	0.33	−1.36	−1.46	100	−1.41
	Reduction 2	0.35	−1.98	−2.17	191	−2.08
			−0.53	—	—	
3	Oxidation 1	—	+0.51	—	—	—
	Oxidation 2	0.71	+0.86	+0.80	52	+0.83
	Reduction 1	0.87	−1.14	−1.20	60	−1.17
	Reduction 2	—	—	−1.88	—	—
	Reduction 3	1.13	−1.99	−2.06	69	−2.02
4	Oxidation 1	—	+0.43	—	—	—
	Oxidation 2	0.83	+0.81	+0.75	55	+0.78
	Reduction 1	1.00	−1.22	−1.28	55	−1.25
	Reduction 2	—	—	−1.98	—	—
	Reduction 3	1.37	−2.06	−2.14	70	−2.10

* All potentials are quoted relative to the ferrocenium–ferrocene couple taken as 0.0 V. Ferrocene was added to the cell for each measurement. Scan rate 0.2 V s^{-1}.

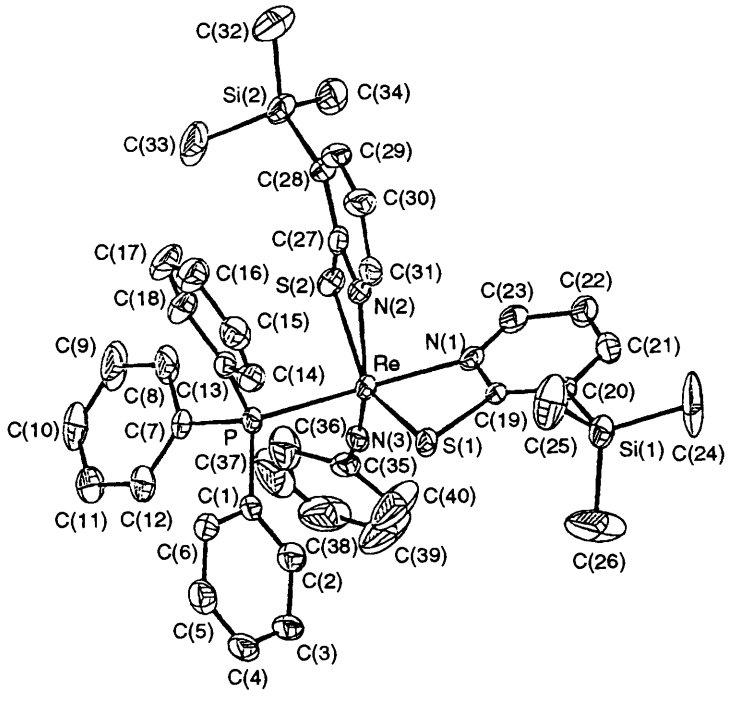

Fig. 3 Perspective view of $[Re(NPh)(PPh_3)(tspys)_2][BPh_4]$ **3** showing the atom labelling scheme

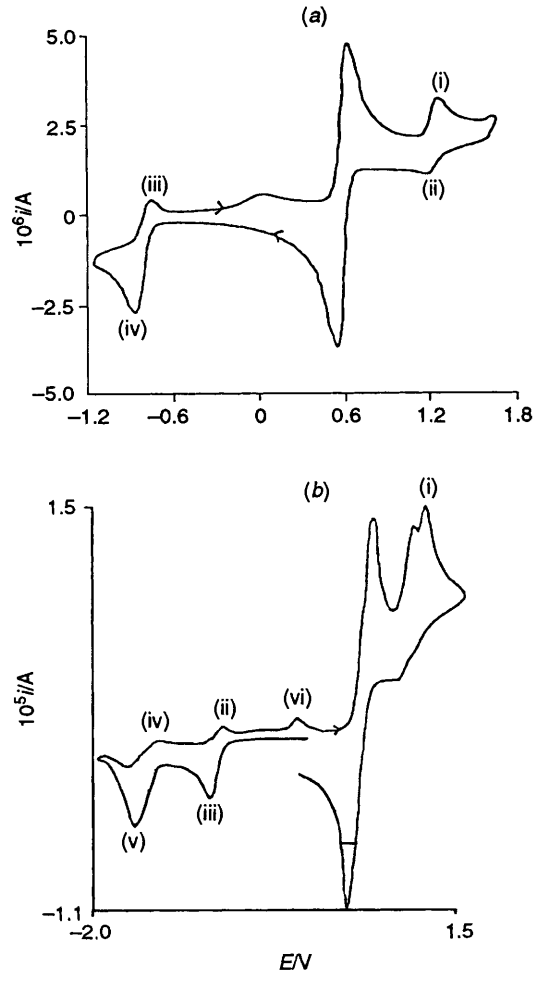

Fig. 4 Cyclic voltammograms for (*a*) $[ReCl_2(NC_6H_4PPh_2\text{-}2)(HNC_6H_4PPh_2\text{-}2)]$ **1** and (*b*) $[Re(8\text{-}HNC_9H_6N)_2O(PPh_3)][BPh_4]$ **2** recorded at room temperature in CH_2Cl_2 at a platinum-wire auxiliary electrode and silver-wire pseudo-reference electrode

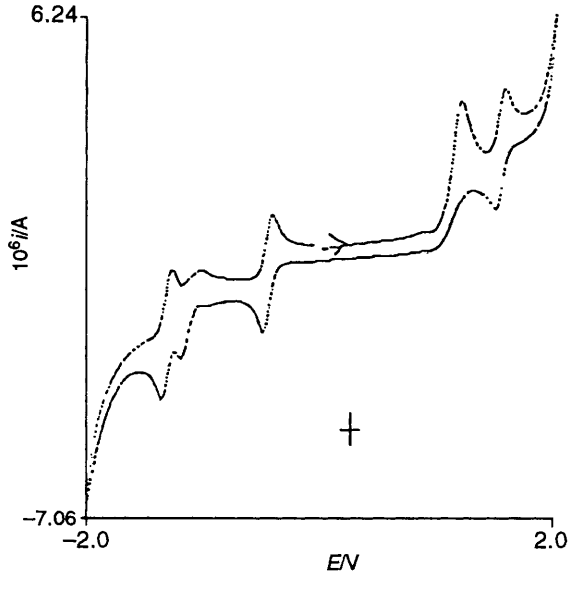

Fig. 5 Cyclic voltammogram for $[Re(NPh)(PPh_3)(tspyt)_2][BPh_4]$ **3** recorded at room temperature in CH_2Cl_2 at a platinum-wire auxiliary electrode and silver-wire pseudo-reference electrode

borate under the same conditions. On the negative potential sweep complex **2** displayed two quasi-reversible reduction processes, the second of which involves a coupled chemical reaction as shown by the presence of the associated broad peak at $E_{pa} = -0.53$ V which is due to the products of the chemical reaction. The first reduction process indicated that the neutral rhenium(IV) species, $[Re(8\text{-}HNC_9H_6N)_2O(PPh_3)]$, has limited stability.

The cyclic voltammogram of $[Re(NPh)(PPh_3)(tspyt)_2][BPh_4]$ **3** is shown in Fig. 5. That of $[Re(NPh)(PPh_3)(pyt)_2][BPh_4]$ **4** is identical although there is a slight lowering of potentials due to the electron-donating silyl substituents. In the positive potential sweep one irreversible and one reversible oxidation process were observed. On the negative potential sweep one irreversible reduction and two reversible reduction processes were identified. The irreversible oxidation corresponds to oxidation of the BPh_4^- counter ion, the reversible oxidation to the formation of a rhenium(VI) dication. The reduction processes correspond to the formation of a neutral rhenium(IV), monoanionic rhenium(III) and dianionic rhenium(II) species. The Re^{IV}–Re^{III} process is only partially reversible even at low temperatures.

Conclusion

We have demonstrated the synthesis and properties of some new rhenium imido-complexes: $[ReCl_2(NC_6H_4PPh_2\text{-}2)(HNC_6H_4PPh_2\text{-}2)]$ represents a new class of complex containing a P,N chelated imide ligand; $[Re(8\text{-}HNC_9H_6N)_2O(PPh_3)][BPh_4]$ **2** was an unexpected product with the 8-aminoquinoline ligands acting as N,N chelated amides; $[Re(NPh)(PPh_3)L_2][BPh_4]$, where L = tspyt **3** or pyt **4**, represents a new class of complexes containing the rhenium imido-core with pyridinethiol coligands. Further studies of the substitution chemistry and electrochemistry of representative complexes of these types will be reported at a later date.

Experimental

All manipulations were carried out under an inert atmosphere of dry dinitrogen gas unless stated otherwise. Standard Schlenk-tube and vacuum-line techniques were employed throughout where appropriate. Elemental analyses were performed by Medac Ltd, University of Brunel. Infrared spectra were measured in the range 200–4000 cm^{-1} as Nujol mulls (KBr plates) on a Perkin-Elmer 1600 series FTIR spectrophotometer, ^1H and $^{31}P\text{-}\{^1H\}$ NMR spectra using a JEOL EX270 MHz spectrometer by Mrs. J. Warmsley and fast atom bombardment mass spectra from the University College Swansea using 3-nitrobenzyl alcohol as a matrix. All materials and reagents were obtained commercially (Aldrich) and used without further purification. The compounds $[ReCl_3O(PPh_3)_2]$,[1] $[ReCl_3(NPh)(PPh_3)_2]$,[23] Htspyt[24] and $2\text{-}Ph_2PC_6H_4NH_2$[25] were prepared using published procedures. The electrochemistry of all the complexes was performed in dichloromethane solution at a platinum-wire working electrode with 0.2 mol dm^{-3} $[NBu^n_4][BF_4]$ as the supporting electrolyte. Potentials were quoted relative to the ferrocene–ferrocenium couple, which was taken as 0.0 V.

Preparation of the Complexes.—$[ReCl_2(NC_6H_4PPh_2\text{-}2)(HNC_6H_4PPh_2\text{-}2)]$ **1**.* The complex $[ReCl_3O(PPh_3)_2]$ (0.40 g, 0.48 mmol) and $2\text{-}Ph_2PC_6H_4NH_2$ (0.40 g, 1.44 mmol) were heated under reflux in toluene (30 cm^3) for 10 min. The resulting dark orange-brown solution was cooled and the solvent removed *in vacuo*. The residue was triturated with Et_2O to yield a brown solid which was filtered off, washed with Et_2O and dried under vacuum. Yield 0.32 g, 82%. Recrystallisation from CH_2Cl_2–Et_2O afforded light brown crystals. IR (KBr)

* *Note added at proof.* The synthesis and structure of $[ReCl_2(NC_6H_4PPh_2\text{-}2)(HNC_6H_4PPh_2\text{-}2)]$ have been reported.[26]

Table 5 Crystallographic data * for complexes **1–3**

	1	**2**	**3**
Formula	$C_{36}H_{29}Cl_2N_2P_2Re$	$C_{60}H_{49}BN_4OPRe$	$C_{64}H_{64}BN_3PReS_2Si_2$
M	808.65	1070.07	1223.46
Crystal size/mm	0.30 × 0.20 × 0.12	0.15 × 0.30 × 0.65	0.40 × 0.25 × 0.15
Crystal shape	Plate	Plate	Needle
a/Å	10.092(1)	9.657(2)	12.838(6)
b/Å	11.533(3)	13.726(4)	13.902(8)
c/Å	14.958(2)	19.407(4)	19.851(8)
α/°	96.23(1)	79.82(2)	106.71(4)
β/°	97.02(2)	78.47(2)	99.88(8)
γ/°	107.97(1)	77.85(2)	110.94(7)
U/Å^3	1623.8(5)	2439.6(1)	3016(3)
D_c/g cm^{-3}	1.654	1.457	1.347
T/K	293(2)	291	293(2)
Reflections collected	6839	9153	6398
Unique data	4844	8597	6080
Observed reflections	4844	7500	6080
h,k,l ranges	$[I > 2\sigma(I)]$ −11 to 10, −13 to 10, −10 to 18	$[F_o \geqslant 3\sigma(F_o)]$ −11 to 0, −16 to 16, −23 to 23	$[I > 2\sigma(I)]$ −16 to 13, −17 to 18, −16 to 23
θ Range for data collection/°	2.35–26.65	1.5–25	2.22–28.00
F(000)	796	1080	1248
R_{int}	0.0319	0.025	0.0523
μ(Mo-Kα)	4.033	2.600	2.190
Absorption correction factors	0.924–1.034	0.49–0.99	0.914–1.028
Correction method	DIFABS [32]	ψ Scans	DIFABS [32]
$R1$	0.028	0.055	0.028
$wR2$	0.072	0.069	0.069
Largest difference peak and hole/e Å^{-3}	1.53, −0.80	3.22, −0.20	0.30, −0.26

* Details in common: triclinic, space group $P\bar{1}$; $Z = 2$; Mo-Kα radiation (λ 0.710 69 Å); scan mode ω–2θ. Data were collected on a Delft Instruments FAST TV area detector diffractometer for structures **1** and **3** and on a Enraf-Nonius CAD4 diffractometer for **2**. Weighting schemes used were as follows: **1**, $w = 1/[\sigma^2(F_o)^2 + (0.0489P)^2 + 0.6770P]$ where $P = [\max(F_o^2 + 2F_c^2)]/3$; **2**, $w = 1/[\sigma^2(F_o)^2 + (0.02F_o)^2]$; **3**, $w = 1/\sigma^2(F_o)^2$. $R1 = \Sigma|F_o - F_c|/F_o$; for **1** and **3** $wR2 = [\Sigma w(F_o^2 - F_c^2)^2/\Sigma w(F_o^2)^2]^{\frac{1}{2}}$ and for **2** $wR2 = [\Sigma w(|F_o| - |F_c|)^2/\Sigma wF_o^2]^{\frac{1}{2}}$.

Table 6 Fractional atomic coordinates (× 10^4) for $[ReCl_2(NC_6H_4PPh_2\text{-}2)(HNC_6H_4PPh_2\text{-}2)]$ **1**

Atom	x	y	z	Atom	x	y	z
Re	1862.1(1)	4851.5(1)	3281.1(1)	C(16)	2773(4)	9624(2)	4716(2)
P(1)	3514(1)	6600(1)	2789(1)	C(17)	2108(3)	8379(2)	4734(2)
P(2)	1807(1)	3012(1)	2218(1)	C(18)	2370(3)	7491(2)	4140(2)
Cl(1)	32(1)	3605(1)	3992(1)	C(19)	1700(4)	2874(3)	985(2)
Cl(2)	57(1)	4920(1)	2116(1)	C(20)	1366(4)	1731(2)	444(2)
N(1)	1729(4)	6232(3)	4145(3)	C(21)	1316(5)	1655(3)	−494(2)
N(2)	3275(4)	4417(3)	3771(2)	C(22)	1600(5)	2722(3)	−891(2)
C(1)	5306(2)	6576(3)	3114(2)	C(23)	1934(4)	3865(3)	−350(2)
C(2)	5845(3)	5867(3)	2541(2)	C(24)	1984(4)	3941(2)	588(2)
C(3)	7168(3)	5768(3)	2812(2)	C(25)	488(3)	1592(2)	2377(2)
C(4)	7952(3)	6376(3)	3656(3)	C(26)	−922(3)	1426(3)	2062(2)
C(5)	7414(3)	7084(3)	4229(2)	C(27)	−1975(2)	421(3)	2248(3)
C(6)	6091(3)	7184(3)	3958(2)	C(28)	−1619(3)	−418(3)	2748(3)
C(7)	3472(3)	7136(4)	1680(2)	C(29)	−209(4)	−252(3)	3063(3)
C(8)	2227(3)	7278(5)	1277(3)	C(30)	845(3)	754(3)	2878(3)
C(9)	2160(4)	7702(6)	443(3)	C(31)	3512(2)	2899(3)	2675(2)
C(10)	3339(5)	7984(7)	12(3)	C(32)	4287(3)	2210(3)	2311(2)
C(11)	4585(4)	7842(6)	414(3)	C(33)	5591(3)	2282(3)	2784(2)
C(12)	4651(3)	7418(5)	1248(3)	C(34)	6120(3)	3042(3)	3621(2)
C(13)	3296(3)	7850(2)	3529(2)	C(35)	5345(3)	3731(3)	3985(2)
C(14)	3960(3)	9096(2)	3511(2)	C(36)	4041(3)	3659(2)	3512(2)
C(15)	3698(3)	9983(2)	4105(2)	H(1)	1148(50)	5972(41)	4434(31)

700–750m (CH), 3260w (NH) and 1435m (PC) cm^{-1}. NMR ($CDCl_3$): ^{1}H, δ 6.1–7.8 (m, Ph H); ^{31}P-{^{1}H}, δ 14 (s) and −4 (s) (Found: C, 53.4; H, 3.6; N, 3.4. $C_{36}H_{29}Cl_2N_2P_2Re$ requires C, 53.5; H, 3.6; N, 3.5%). FAB mass spectrum: m/z, 808 {100, $[ReCl_2(NC_6H_4PPh_2)(HNC_6H_4PPh_2)]^+$} and 773 {42%, $[ReCl(NC_6H_4PPh_2)(HNC_6H_4PPh_2)]^+$}.

$[Re(8\text{-}HNC_9H_6N)_2O(PPh_3)][BPh_4]$ **2**. The complex $[ReCl_3O(PPh_3)_2]$ (0.50 g, 0.60 mmol) and 8-aminoquinoline (1.33 g, 8.98 mmol) were heated under reflux in ethanol (30 cm^3) for 4 h. The resulting dark brown solution was cooled and the volume reduced under vacuum to 10 cm^3. A solution of $NaBPh_4$ (0.20 g, 0.60 mmol) in methanol (2 cm^3) was added to precipitate the complex as a brown microcrystalline solid which was filtered off, washed with Et_2O and dried under vacuum. Yield 0.40 g, 71%. Recrystallisation from CH_2Cl_2–MeOH afforded light brown crystals. IR (KBr) 897s (Re=O), 3273w and 3314w (NH) cm^{-1}. NMR ($CDCl_3$): ^{1}H, δ 6.6–8.0 (m, Ph H); ^{31}P-{^{1}H}, δ 4.4 (s) (Found: C, 67.4; H, 4.5; N, 5.3. $C_{60}H_{49}BN_4OPRe$ requires C, 67.3; H, 4.6; N, 5.2%). FAB mass spectrum: m/z, 751 {38, $[Re(8\text{-}HNC_9H_6N)_2O(PPh_3)]^+$} and 489 {70%, $[Re(8\text{-}HNC_9H_6N)_2O]^+$}.

$[Re(NPh)(PPh_3)(tspyt)_2][BPh_4]$ **3**. The complex [Re-

Table 7 Fractional atomic coordinates for $[Re(8\text{-}HNC_9H_6N)_2O(PPh_3)][BPh_4]$ **2**

Atom	*x*	*y*	*z*	Atom	*x*	*y*	*z*
Re	0.168 26(3)	0.187 99(2)	0.283 24(1)	C(44)	−0.160(1)	0.490 0(9)	0.080 1(6)
P	0.174 4(2)	0.222 1(1)	0.155 01(9)	C(45)	−0.118(1)	0.408 5(8)	0.040 9(6)
O	0.316 6(5)	0.096 1(4)	0.268 6(3)	C(46)	−0.015 8(9)	0.326 1(8)	0.062 7(5)
N(1)	0.043 8(6)	0.070 0(4)	0.290 1(3)	C(51)	0.155 1(7)	0.111 8(6)	0.120 3(4)
N(2)	−0.040 5(6)	0.256 0(5)	0.303 8(3)	C(52)	0.019 5(9)	0.091 0(7)	0.124 2(4)
N(3)	0.180 0(6)	0.166 7(5)	0.394 9(3)	C(53)	0.011(1)	−0.004 1(8)	0.104 2(6)
N(4)	0.229 0(6)	0.312 8(5)	0.290 2(3)	C(54)	0.131(1)	−0.069 3(7)	0.082 6(6)
C(11)	0.097 1(8)	−0.027 2(6)	0.283 4(4)	C(55)	0.263(1)	−0.047 7(8)	0.079 8(6)
C(12)	0.007 7(9)	−0.098 0(7)	0.283 7(5)	C(56)	0.279(1)	0.045 4(7)	0.097 1(5)
C(13)	−0.141 3(8)	−0.064 0(6)	0.290 7(4)	C(61)	0.338 1(8)	0.384 2(6)	0.687 6(4)
C(14)	−0.199 9(7)	0.034 1(6)	0.300 7(4)	C(62)	0.197 0(9)	0.365 6(8)	0.704 8(5)
C(15)	−0.348 5(8)	0.074 6(7)	0.310 6(5)	C(63)	0.086(1)	0.433(1)	0.671 9(6)
C(16)	−0.394 5(8)	0.177 3(8)	0.318 6(5)	C(64)	0.116(1)	0.516 0(8)	0.622 5(5)
C(17)	−0.296 2(8)	0.240 1(7)	0.316 8(5)	C(65)	0.254(1)	0.534 6(7)	0.605 9(5)
C(18)	−0.151 7(7)	0.201 8(5)	0.307 1(3)	C(66)	0.363 4(9)	0.469 0(6)	0.639 1(5)
C(19)	−0.102 1(7)	0.099 9(5)	0.299 7(3)	C(71)	0.421 6(8)	0.216 8(6)	0.780 5(4)
C(21)	0.156(1)	0.088 4(7)	0.442 9(4)	C(72)	0.466 8(8)	0.114 8(6)	0.774 1(5)
C(22)	0.177(1)	0.083 7(8)	0.516 1(5)	C(73)	0.422(1)	0.038 8(7)	0.826 9(5)
C(23)	0.211(1)	0.168 9(8)	0.535 0(5)	C(74)	0.330(1)	0.064 6(8)	0.888 8(5)
C(24)	0.231 6(8)	0.254 0(6)	0.483 6(4)	C(75)	0.283(1)	0.162 8(8)	0.896 8(5)
C(25)	0.269(1)	0.340 7(7)	0.499 0(4)	C(76)	0.328(1)	0.239 2(8)	0.842 7(5)
C(26)	0.294(1)	0.417 1(8)	0.445 3(5)	C(81)	0.585 2(9)	0.269 5(6)	0.650 4(4)
C(27)	0.282 9(9)	0.412 9(6)	0.373 1(4)	C(82)	0.721(1)	0.297 7(8)	0.626 1(5)
C(28)	0.245 2(7)	0.328 2(6)	0.358 2(4)	C(83)	0.807(1)	0.264 9(9)	0.561 4(6)
C(29)	0.217 7(7)	0.250 0(5)	0.413 3(4)	C(84)	0.756(2)	0.204 9(9)	0.523 6(6)
C(31)	0.346 5(7)	0.251 0(6)	0.104 4(4)	C(85)	0.623(1)	0.179 9(9)	0.547 4(6)
C(32)	0.466 6(8)	0.233 1(6)	0.137 0(4)	C(86)	0.536(1)	0.208 9(8)	0.610 7(5)
C(33)	0.598 1(8)	0.249 2(7)	0.095 8(5)	C(91)	0.553 0(8)	0.370 8(6)	0.763 8(4)
C(34)	0.608(1)	0.280 0(8)	0.024 9(6)	C(92)	0.491 2(9)	0.467 3(6)	0.782 3(5)
C(35)	0.489(1)	0.298 7(9)	−0.009 4(5)	C(93)	0.558(1)	0.512 3(7)	0.821 9(5)
C(36)	0.359 6(9)	0.284 0(8)	0.031 6(5)	C(94)	0.685(1)	0.465 6(9)	0.845 5(5)
C(41)	0.039 3(8)	0.327 1(6)	0.124 1(4)	C(95)	0.748(1)	0.370 1(9)	0.827 9(5)
C(42)	−0.001 7(9)	0.407 5(6)	0.161 8(5)	C(96)	0.677 1(9)	0.323 5(8)	0.789 4(5)
C(43)	−0.103(1)	0.489 5(8)	0.140 0(6)	B	0.473 9(9)	0.311 1(7)	0.720 7(5)

Table 8 Fractional atomic coordinates (× 10^4) for $[Re(NPh)(PPh_3)(tspyt)_2][BPh_4]$ **3**

Atom	*x*	*y*	*z*	Atom	*x*	*y*	*z*
Re	554.5(4)	3952.6(4)	1611.3(2)	C(30)	1661(11)	5430(10)	4101(6)
P	2627(2)	4857(2)	1732(1)	C(31)	1355(8)	5399(9)	3398(6)
S(1)	276(2)	5578(2)	1709(2)	C(32)	1983(12)	2586(13)	4768(7)
S(2)	589(2)	2481(2)	2054(2)	C(33)	2779(11)	2177(12)	3414(9)
Si(1)	−1914(3)	6508(3)	2114(2)	C(34)	225(10)	973(10)	3291(7)
Si(2)	1568(3)	2287(3)	3763(2)	N(3)	173(7)	3071(7)	706(4)
C(1)	2918(6)	5803(5)	1232(3)	C(35)	−106(8)	2183(6)	56(4)
C(2)	2077(5)	5528(5)	580(4)	C(36)	556(7)	1577(8)	−1(5)
C(3)	2308(6)	6175(7)	157(3)	C(37)	244(10)	664(8)	−644(6)
C(4)	3380(7)	7097(6)	386(4)	C(38)	−730(11)	355(8)	−1230(5)
C(5)	4221(5)	7371(5)	1039(4)	C(39)	−1392(10)	961(10)	−1174(5)
C(6)	3990(5)	6724(6)	1462(3)	C(40)	−1079(9)	1875(9)	−530(5)
C(7)	3262(6)	3925(6)	1337(4)	B	6249(10)	869(10)	3258(7)
C(8)	3202(7)	3076(6)	1588(4)	C(41)	6711(6)	2242(5)	3493(4)
C(9)	3677(8)	2356(6)	1298(5)	C(42)	5929(5)	2719(7)	3551(4)
C(10)	4211(7)	2484(7)	756(5)	C(43)	6308(8)	3848(7)	3693(5)
C(11)	4271(7)	3333(8)	506(4)	C(44)	7468(9)	4500(5)	3777(4)
C(12)	3796(7)	4054(6)	796(4)	C(45)	8250(6)	4024(6)	3719(4)
C(13)	3543(5)	5705(5)	2685(3)	C(46)	7872(6)	2895(7)	3577(4)
C(14)	3615(6)	6768(5)	2997(4)	C(47)	4914(5)	264(5)	3370(4)
C(15)	4245(7)	7416(5)	3737(4)	C(48)	4842(5)	622(5)	4083(3)
C(16)	4802(6)	7001(6)	4164(3)	C(49)	3787(6)	152(6)	4220(3)
C(17)	4729(6)	5938(6)	3852(4)	C(50)	2805(5)	−676(6)	3645(5)
C(18)	4099(6)	5290(5)	3113(4)	C(51)	2877(5)	−1034(5)	2932(4)
N(1)	−1075(6)	3795(6)	1770(4)	C(52)	3932(6)	−564(6)	2795(3)
C(19)	−1060(8)	4791(8)	1832(5)	C(53)	7145(6)	579(6)	3803(3)
C(20)	−1954(8)	5088(8)	1963(5)	C(54)	6967(6)	−523(5)	3618(4)
C(21)	−2913(9)	4238(10)	1986(6)	C(55)	7649(7)	−806(6)	4078(5)
C(22)	−2961(9)	3213(10)	1924(6)	C(56)	8509(6)	14(8)	4723(4)
C(23)	−2017(9)	3008(9)	1803(6)	C(57)	8687(6)	1116(7)	4908(3)
C(24)	−3234(11)	6531(13)	2345(10)	C(58)	8005(6)	1399(5)	4448(4)
C(25)	−604(12)	7578(12)	2914(9)	C(59)	6240(7)	414(6)	2368(3)
C(26)	−1881(21)	6764(15)	1252(9)	C(60)	7093(6)	95(7)	2178(4)
N(2)	1069(7)	4469(6)	2806(4)	C(61)	7140(8)	−163(7)	1457(5)
C(27)	1042(8)	3530(8)	2913(5)	C(62)	6334(10)	−101(7)	926(3)
C(28)	1388(9)	3506(9)	3625(6)	C(63)	5480(8)	218(7)	1115(4)
C(29)	1667(10)	4480(10)	4190(6)	C(64)	5433(6)	475(7)	1837(5)

$Cl_3(NPh)(PPh_3)_2$] (0.31 g, 0.34 mmol) and Htspyt (0.17 g, 0.93 mmol) were heated under reflux in ethanol (15 cm^3) for 30 min. The resulting dark green solution was filtered to remove any solid impurities. Addition of $NaBPh_4$ (0.12 g, 0.34 mmol) resulted in the immediate precipitation of [Re(NPh)(PPh_3)-(tspyt)$_2$][BPh_4] **3** as a dark green solid which was filtered off and washed with Et_2O. Recrystallisation from CH_2Cl_2–EtOH afforded dark green needles. Yield 0.30 g, 70%. IR (KBr) 1550s (SN), 840, 1470s (CSi) and 1155m (CS) cm^{-1}. NMR ($CDCl_3$): ^1H, δ 6.2–8.0 (m, Ph H) and 0.7 [18 H, 2 s, $Si(CH_3)_3$]; ^{31}P-{^1H}, δ 12.3 (s) (Found: C, 62.3; H, 5.2; N, 3.4. $C_{64}H_{64}BN_3PReS_2Si_2$ requires C, 62.8; H, 5.2; N, 3.4%). FAB mass spectrum: *m*/*z*, 904 {100 [Re(NPh)(PPh_3)(tspyt)$_2$]$^+$}, 722 {55, [Re(NPh)(PPh_3)-(tspyt)]$^+$}, 542 {100, [ReN(PPh_3)(tspyt)]$^+$} and 460 {77, [ReN(PPh_3)]$^+$}.

[Re(NPh)(PPh_3)(pyt)$_2$][BPh_4] **4**. The procedure outlined for the synthesis of complex **3** was followed using [Re-Cl_3(NPh)(PPh_3)$_2$] (0.20 g, 0.22 mmol), Hpyt (0.12 g, 1.10 mmol) and $NaBPh_4$ (0.07 g, 0.22 mmol). Yield of [Re-(NPh)(PPh_3)(pyt)$_2$][BPh_4] 0.16 g, 70%. IR (KBr) 1580s (SN), 840m and 1160m (CS) cm^{-1}. NMR ($CDCl_3$): ^1H, δ 6.0–8.7 (m, Ph H); ^{31}P-{^1H} δ 13.2 (s) (Found: C, 64.5; H, 4.4; N, 3.6. $C_{53}H_{44}BN_3PReS_2$ requires C, 64.6; H, 4.5; N, 3.9%).

X-Ray Crystallography.—Structure analysis and refinement. Structures **1** and **3** were solved by direct methods (SHELXS)[27] and refined on F_o^2 (SHELXL 93)[28] using all unique F_o^2 data corrected for Lorentz and polarisation factors. Structure **2** was solved by the Patterson heavy-atom method[29] followed by successive cycles of Fourier-difference syntheses[30] and full-matrix least squares on $|F_o|$. The hydrogen atoms were included in calculated positions but not refined, except for H(1) for structure **1** which was found in a difference synthesis and refined isotropically. Neutral atomic scattering factors were used.[31] The experimental details of the data collections and structure solutions are summarized in Table 5, final atomic coordinates in Tables 6–8.

Additional material available from the Cambridge Crystallographic Data Centre comprises H-atom coordinates, thermal parameters and remaining bond lengths and angles.

Acknowledgements

We thank the SERC for a CASE award with Amersham International plc (to B.C.). The authors gratefully acknowledge the Hermann Stark Company, Germany for their generous gift of rhenium metal.

References

1 J. Chatt and G. J. Rowe, *J. Chem. Soc.*, 1962, 4019.
2 T. Nicholson, S. L. Storm, W. M. Davis, A. Davison and A. G. Jones, *Inorg. Chim. Acta*, 1992, **196**, 27.
3 P. J. Blower and J. R. Dilworth, *J. Chem. Soc., Dalton Trans.*, 1985, 2305.
4 G. V. Goeden and B. L. Haymore, *Inorg. Chem.*, 1983, **22**, 157.
5 G. K. Lahiri, S. Goswami, L. R. Falvello and A. Chakravorty, *Inorg. Chem.*, 1987, **26**, 3365.
6 G. R. Clarke, A. J. Nielson and C. E. F. Rickard, *Polyhedron*, 1988, **7**, 117.
7 M. R. Cook, W. A. Herrmann, P. Kiprok and J. Takacs, *J. Chem. Soc., Dalton Trans.*, 1991, 797.
8 A. A. Danopoulos, G. Wilkinson, B. Hussain and M. B. Hursthouse, *J. Chem. Soc., Chem Commun.*, 1989, 896.
9 R. Torecki, R. R. Schrock and W. M. Davis, *J. Am. Chem. Soc.*, 1992, **114**, 3367.
10 B. Coutinho and J. R. Dilworth, unpublished work.
11 A. D. Horton, R. R. Schrock and J. H. Freundenberger, *Organometallics*, 1987, **6**, 893.
12 M. H. Scholfield, R. R. Schrock and L. Y. Park, *Organometallics*, 1991, **10**, 1844.
13 O. D. Sloan and P. Thornton, *Polyhedron*, 1988, **7**, 329.
14 M. K. Cooper and J. M. Downes, *Inorg. Chem.*, 1978, **17**, 880.
15 C. W. G. Ansell, M. McPartlin, P. A. Tasker, M. K. Cooper and P. A. Duckworth, *Inorg. Chim. Acta*, 1983, **76**, L135.
16 F. Refosco, T. Tisato, G. Bandoli, C. Bolzati, A. Dolmella, A. Moresco and M. Nicolini, *J. Chem. Soc., Dalton Trans.*, 1993, 605.
17 F. Refosco, G. Bandoli, C. Bolzati, A. Dolmella, A. Moresco, U. Mazzi and M. Nicolini, *J. Chem. Soc., Dalton Trans.*, 1991, 3043.
18 C. Lu, J. R. Dilworth and J. R. Miller, unpublished work.
19 J. L. Fourquet, M. Leblanc, A. Saravanamuthu, M. R. M. Bruce and A. E. Bruce, *Inorg. Chem.*, 1991, **30**, 3241.
20 E. Block, M. Gernon, H. Kang, G. Ofori-Okai and J. A. Zubieta, *Inorg. Chem.*, 1991, **30**, 1747.
21 B. L. Haymore, *J. Am. Chem. Soc.*, 1979, **101**, 2063.
22 C. M. Archer, J. R. Dilworth, P. Jobanputra, M. E. Harman, M. B. Hursthouse and A. Karulov, *Polyhedron*, 1991, **10**, 1539.
23 J. Chatt, J. R. Dilworth and G. J. Leigh, *J. Chem. Soc. A*, 1970, 2239.
24 E. Block, M. Gernon, H. Kang, G. Ofori-Okai and J. A. Zubieta, *Inorg. Chem.*, 1991, **30**, 34.
25 P. A. Duckworth, M. K. Cooper, J. M. Downes, M. C. Kerby, R. J. Powell and M. D. Soucek, *Inorg. Synth.*, 1989, **27**, 129.
26 F. Refosco, F. Tisato, A. Moresco, A. Cagnolini, G. Bandoli and C. Bolzati, *Technetium and Rhenium in Chemistry and Nuclear Medicine*, eds. M. Nicolini, G. Bandoli and U. Mazzi, S. G. Editoriali, Padova, Italy, 1995.
27 G. M. Sheldrick, *Acta Crystallogr., Sect. A*, 1990, **46**, 467.
28 G. M. Sheldrick, University of Göttingen, 1993.
29 J. C. Calbrese, PhD. Thesis, PHASE, Patterson Heavy Atom Solution Extractor, University of Wisconsin, Madison, 1972.
30 MOLEN, An Interactive Structure Solution Procedure, Enraf-Nonius, Delft, 1990.
31 D. T. Cromer and J. T. Waber, *International Tables for X-Ray Crystallography*, Kynoch Press, Birmingham, 1974, vol. 4, Table 2.3.1.
32 DIFABS, N. G. Walker and D. Stuart, *Acta Crystallogr., Sect. A*, 1983, **39**, 158.

Received 10*th March* 1995; *Paper* 5/01479D